



MEDICINAL PLANT EXTRACTS USED FOR BLOOD SUGAR AND OBESITY THERAPY SHOWS EXCELLENT INHIBITION OF INVERTASE ACTIVITY: SYNTHESIS OF NANOPARTICLES USING THIS EXTRACT AND ITS CYTOTOXIC AND GENOTOXIC EFFECTS

VIRGINIA D'BRITTO¹, PHILEM PUSHPARANI DEVI¹, B. L. V. PRASAD², ALOK DHAWAN³, VIVEK G. MANTRI³ AND ASMITA PRABHUNE^{1,*}

¹ Biochemical Sciences Division, National Chemical Laboratory, Pune-411 008.

² Physical Chemistry Division, National Chemical Laboratory, Pune-411 008.

³ Indian Institute of Toxicology Research, Lucknow-226 001.

⁴ Mantri Homeopathy Clinic, Pune-411 009.

ABSTRACT

Extract of *Azardirecta indica*, *Cephalandra indica*, *Calotropis procera* and *Syzygium jambolanum*, prepared together, is an elixir for the treatment of blood sugar and obesity in homoeopathic medicine. Like many other homeopathic elixir, the exact mechanism of action of this popular elixir is also still unknown. It is known that inhibitors of α -glucosidases such as invertase, α amylase etc, can delay the digestion and adsorption of carbohydrates, thereby, inhibiting post prandial hyperglycemia and thus helps in Diabetes therapy. In our present study, the invertase inhibitor action of the elixir was tested in order put more light on the therapeutic mechanism of this elixir. Moreover, rapid bio-reduction of Au^{3+} and Ag^+ ions to their respective nanoparticles was achieved using the same extract of these medicinal plants. Cytotoxicity (MTT assay) and genotoxicity (COMET assay) experiments have been performed on these nanomaterials. Invertase inhibition activity was excellent. MTT results proved the bio-compatible nature of these biochemically synthesized gold and silver nanoparticles upto 10^{-4}M concentration towards HepG2 cells. At higher nanoparticle concentration (10^{-3}M or above), DNA damage occurred which was very easily detected by COMET assay. The overall study suggested that these biogenic metal nanoparticles are non-cytotoxic and non-genotoxic upto 10^{-4}M .

Keywords: Homeopathic medicine, Invertase inhibition, Bioreduction, Cytotoxicity, Genotoxicity

INTRODUCTION

Traditional medicinal practitioners have been using numerous plants and their extracts for therapy since time immemorial. It is universal that such plant based products are eco-friendly, bio-friendly and hence are more safe and effective than synthetic drugs. However, the exact mechanism of action or the active principle(s) responsible for such therapeutic effect of many popular and common plant based elixir are still undefined. In order to promote herbal medicine, more investigations need to be done on the mode

of action of such medicine with complex composition.

Apart from medical application, recently with the commence of the age of nanotechnology, plant extract find its application as a safe, 'green approach' based nanoparticle synthesizing agent (Lakin HW et al., 1974; Gardea-Torresdey JL et al. 2002; Torresdey JLG et al. 2003; Shankar SS et al. 2003a; Shankar SS et al. 2003b; Shankar SS, 2004a; Shankar SS et al. 2004b; Shankar SS et al. 2005; Ankamwar B et.al 2005; Huang J et al.

2007; Chandran SP et al. 2006; Sharma NC et al. 2007; Nune SK et al. 2009; Ogi T et al. 2009). Since many of the medical and biological applications of nanoparticles are typically based on their interactions with bio-molecules, in all circumstances, it becomes very important to access the toxic effects of these nanoparticles prior to their exposure to the human body. Nanoparticles are known to accumulate at particular locations i.e. vesicles, mitochondria from where they can exert toxic responses. Particles with smaller size have larger surface area and thus would involve in generation of a substantial amount of reactive oxygen species (ROS), which play a major role in nanoparticle toxicity (Nel A et al, 2006). In this regard, Dunford et al. (1997) studied genotoxicity of human fibroblast cells and reported that TiO_2/ZnO nanoparticles from sunscreen were found to induce generation of free radicals and catalyzed DNA damage both in cell free system and *in vitro*.

In our present study, an elixir prepared from four medicinal plants, *Azardirecta indica*, *Cephalandra indica*, *Calotropis procera* and *Syzygium jambolanum*, used for the treatment of blood sugar and obesity in homoeopathic medicine, has been explored for its therapeutic mechanism and bio-reducibility of metal ions to nanoparticles. The treatment for diabetes involves an inhibitory regulation of α -glucosidases which hydrolyze the α -glucoside linkages of sucrose and storage carbohydrates like starch and glycogen to increase blood sugar levels. With this principle in mind, an attempt has been made to explain the anti blood sugar of this elixir by the evaluation of its ability to inhibit invertase activity. The effect of variable exposure time, incubation time and temperature were studied using the elixir and the optima for each were determined.

We described the use of the elixir to synthesize gold nanoparticles (B-AuNPs) and silver

nanoparticles (B-AgNPs). Here 'B' stands for biologically synthesized. Characterization of these nanoparticles was carried out using UV-vis spectroscopy, TEM, XRD and thermogravimetric analysis. We present our results on the cytotoxic and genotoxic effects of the gold nanoparticles (B-AuNPs) and silver nanoparticles (B-AgNPs). MTT assay was performed to study the cytotoxicity, whereas COMET assay was undertaken for genotoxicity evaluation. The synthesis protocol and detailed characterization of B-AuNPs and B-AgNPs along with a comparative discussion about their cytotoxicity and genotoxicity effects on HepG2 (human liver carcinoma) cells have been discussed in detail.

MATERIALS AND METHODS

Ethyl methane sulphonate (EMS; CAS No. 62-50-0), normal melting point agarose (NMA), low melting point agarose (LMPA) and ethidium bromide (EtBr) were purchased from Sigma chemicals (St. Louis, MO). Ca^{+2} and Mg^{+2} ion-free phosphate buffered saline (PBS) was purchased from Hi-Media (Mumbai, India). All other chemicals were obtained locally and were of analytical reagent grade. EMS which is much known for its mutagenic behaviour (Bilbao C 2002) was used as positive control in this study. Sucrose and 3, 5- Dinitrosalicylic acid was obtained from MERCK, India.

1. PREPARATION OF EXTRACTS

The elixir used for treatment of blood sugar and obesity was procured from Dr. V. G. Mantri /Dr Madhuri (homoeopathic practitioner). The extracts were prepared by boiling various parts of the plants in a mixture of ethanol and water. The resultant mother liquor was used in various proportions for the invertase assay and synthesis of nanoparticles.

Table 1: Details of plant composition used in making the elixir.

Name of drug	Part of plants	Water %age	Alcohol %age
<i>Cephalandra Indica</i>	Leaves and fruits	10 to 40	40 to 90
<i>Syigium Jambolanum</i>	Fruit seeds	10 to 40	40 to 90
<i>Calotropis Giganta</i>	Leaves	10 to 40	40 to 90
<i>Axardirachta Indica</i>	Fruit leaf and bark	10 to 40	40 to 90

2. INVERTASE INHIBITION ASSAY

20 μ l (150 μ g) of purified enzyme in 260 μ l of 50 mM acetate buffer pH 4.5 was mixed with 20 μ l of the elixir and incubated for 10 minutes at room temperature. 200 μ l of sucrose (2g%) was added and invertase activity was checked under standard assay conditions, keeping appropriate elixir, alcohol and sucrose blanks as controls (Gascom S and Lampen J0, 1968).

2.1 Effect of variable elixir concentration

The enzyme in buffer, prepared as above, was mixed with various concentrations of the elixir and kept at room temperature for 10 minutes. 200 μ l of sucrose (2g%) was added to each aliquot and invertase activity determined as above. Elixir obtained from homopath was treated as 100%. It was diluted with water to get the desired concentrations ranging from 1:1 to 1:10 dilutions.

2.2 Effect of variable exposure time

The enzyme was suitably diluted as described above with 50 mM acetate buffer and was mixed with the elixir and kept on ice. Aliquots were removed at intervals of 5 minutes, keeping a maximum exposure time of 50 minutes. To each aliquot, 200 μ l of 2g% of sucrose was added. Invertase activity was determined using standard assay procedure keeping appropriate controls.

2.3 Effect of variable incubation time and temperature

The elixir (250 μ l) was added to the enzyme (20 μ l) in 50mM acetate buffer at pH 4.5. Three different temperatures were selected for 10 minutes and 30 minutes exposure time. In the first experiment, the enzyme was incubated with the elixir at 30°C for 10 minutes and aliquot was removed and assayed for invertase activity under standard assay conditions. Another aliquot was removed after 30 minutes. Similar experiment was performed at 40°C and 50°C and corresponding samples were removed as explained above.

3. SYNTHESIS OF B-AUNPS AND B-AGNPs

For preparation of AuNPs, 100 mL of 10⁻⁴ M HAuCl₄ was prepared and 100 μ L of undiluted elixir was added to it. Similarly, AgNPs was prepared from 100 mL of 10⁻⁴ M AgNO₃ and 100 μ L of the elixir. Both the solutions were allowed to

stand for 24 h, to ensure complete reduction of Au³⁺ and Ag⁺ ions to their respective neutral metal states. These nanoparticles were then separated from the solution by means of centrifugation and further characterization was carried out using UV-vis spectroscopy, TEM, XRD and thermogravimetric analysis.

4. CHARACTERIZATION OF B-AUNPS AND B-AGNPs

The UV-visible spectrums of B-AuNPs and B-AgNPs were recorded using JASCO model V-570 dual beam spectrophotometer operated at a resolution of 1 nm. The morphology of the AgNPs was examined using transmission electron microscopy (JEOL model 1200 EXinstrument operated at an accelerating voltage of 80 kV). The XRD sample for B-AuNPs and B-AgNPs was prepared by drop coating the nanoparticle solution onto clean glass slides and analyzed on a Panalytical (XPERTPRO). The amount of capping molecules present along with AuNPs and AgNPs was calculated by thermogravimetric analysis using Rheometric TG Analyser (Rheometric Scientific, USA).

5. CYTOTOXICITY AND GENOTOXICITY ASSESSMENT

5.1 Preparation of different dilutions of B-AuNPs and B-AgNPs

B-AuNPs and B-AgNPs were subjected to dialysis for 24 h against Millipore water using a dialysis bag of 12.5-kDa, cut-off in order to remove excess of plant extract, unreacted Au³⁺ and Ag⁺ ions and other impurities. Further, this nanoparticle solution was concentrated up to 10⁻² M by centrifugation. This solution was considered as stock solution. Lower dilutions of B-AuNPs and B-AgNPs for treatment of HepG2 cells were prepared by diluting the stock solution.

5.1 Cell lines

HepG2 (human hepatocellular carcinoma) cell line was used for cytotoxicity and genotoxicity study of B-AuNPs and B-AgNPs. The HepG2 (ATCC No. HB-8065) cell line was initially procured from National Centre for Cell Science, Pune, India and has been maintained further in Industrial Institute of Toxicology Research, Lucknow, India. The cells were maintained in Complete Modified Eagle Medium (CMEM) supplemented with 10 % Foetal

Bovine Serum (FBS), 1 mM sodium pyruvate, 2 mM glutamine, 50 U/mL penicillin, 50 mg/mL streptomycin and 100 mM non-essential amino acids. Cells were cultured for 3-4 days (~80 % confluence) before the assay.

5.2 Sample Preparation for MTT assay

The above-mentioned stock solution (1 mg/mL) of B-AuNPs and B-AgNPs were used to make the working nanoparticle suspension by serial dilution method. 100 μ L of stock solution of B-AuNPs or B-AgNPs was diluted to 1 mL, thus giving a working nanoparticle suspension of 100 μ g/mL. This solution was further diluted in a similar way. Thus, different B-AuNPs or B-AgNPs concentrations ranging from 10 μ g/mL, 1 μ g/mL, 0.1 μ g/mL, 0.01 μ g/mL, 0.001 μ g/mL and 0.0001 μ g/mL were made in complete Modified Eagle's Medium (CMEM) containing 10% (Foetal Bovine Serum) FBS.

5.3 MTT assay

The MTT assay was performed following the method described by Mosmann (1983) with slight modification. In brief, Hep G2 cells (10,000–15,000 cells/well in 100 μ L of medium) were seeded in a 96-well plate and allowed to adhere for 24 h at 37°C in a 5% CO₂–95% air atmosphere. Medium was replaced with serum-free medium containing B-AuNPs or B-AgNPs ranging from 10 mM to 50 μ M and incubated for 3 h at 37°C. The treatments were discarded and 100 μ L serum-free medium along with 10 μ L MTT (5 mg/mL) in PBS was added to each well and re-incubated for another 3 h at 37 °C. The reaction mixture was then carefully taken out and formazan crystals were solubilised by adding 200 μ L of DMSO to each well and mixing thoroughly. After 10 min, the absorbance of the purple colour was read at 570 nm, using Elisa Reader (SpectraMax 250, Molecular Devices). Untreated polymer films/scaffolds were also run parallel under identical conditions and served as control. The % mitochondrial activity was calculated as

$$(\frac{A_{570} \text{ of treated samples}}{A_{570} \text{ of untreated samples}}) \times 100$$

where A is absorbance at 570 nm. The data presented are the mean \pm SD from three independent experiments.

6. MORPHOLOGICAL ANALYSIS

Morphology of cells before and after the B-AuNPs or B-AgNPs treatment was examined under the

phase-contrast inverted microscope (Leica, Germany). The changes in the cells were quantified using automatic image analysis software Leica Q Win 500, hooked up with the inverted phase-contrast microscope.

7. COMET ASSAY

The COMET assay was performed according to the method described by Singh NP *et al.* (1988) with slight modification. In brief, cell pellets were obtained by centrifugation (5000 rpm, 5 min), which were again resuspended in 100 μ L of PBS. To this 100 μ L of 1 % LMPA (low melting point agar) was added, mixed well at 37 °C and finally layered on top of the end-frosted slides that were precoated with 1 % normal melting point agarose. Now cover slips (24 mm x 60 mm) were placed on top of the slides and were kept at 4 °C. After 5 min the cover slips were removed and 100 μ L of 0.5 % LMPA was again layered on top of the slides before placing the cover slips back and keeping the slides at 4 °C again. After overnight lysis at 4 °C in freshly prepared lysing solution (2.5 M of NaCl, 100 mM of EDTA, 10 mM of Tris and 1 % Triton X-100, pH 10), slides were kept in an electrophoretic unit (Life Technologies, Gaithersburg, MD), filled with chilled and freshly prepared electrophoresis buffer (1 mM Na₂EDTA and 300 mM NaOH, pH ~13). The slides were left (in the electrophoresis solution) for 30 min to allow unwinding of DNA. Following the unwinding, electrophoresis was performed for 30 min at 0.7 V/cm using a power supply from Techno Source (Mumbai, INDIA). To prevent DNA damage from stray light, if any, all the steps starting from single cell preparation were performed under dimmed light. After electrophoresis, the slides were immediately neutralized with 0.4 M of Tris buffer (pH 7.5) for 5 min and the neutralizing process was repeated three times for 5 min each. The slides were then stained with EtBr (20 mg/mL; 75 μ L per slide) for 10 min in dark. After staining, the slides were dipped once in chilled distilled water to remove the excess stain and subsequently, fresh cover slips were kept over them. The slides were examined within 3-4 h, using an image analysis system (Kinetic Imaging, Liverpool, UK) attached to a fluorescent microscope (Leica, Germany). The images were transferred to a computer through a charge coupled device camera and analyzed using Komet 5.0 software. All the experiments were

conducted in triplicates and the slides were prepared in duplicates. Twenty-five cells per slide equalling 150 cells per group were randomly captured at a constant depth of the gel, avoiding the cells present at the edges and superimposed comets.

8. STATISTICAL ANALYSIS

Data were analyzed using Analysis of Variance (ANOVA). The level of statistical significance was set at $P < 0.05$ and $P < 0.01$ wherever required.

RESULTS AND DISCUSSION

Inhibition of invertase activity

The undiluted elixir showed almost 100 % inhibition of invertase activity. Similar inhibition was seen when the elixir was diluted to 1:1 ratio.

There was 60% lost of activity of the enzyme when the elixir was diluted to 1:10 ratio as described in Table 1.

It was seen that exposure time did not show any significant changes in the % inhibition (Table 2). Therefore, the binding of the inhibitor(I) compound to the enzyme (E), which would form the EI complex, seems to be more or less instantaneous. However, at 50°C maximum inhibition was observed (Figure 1). It was speculated that, an enzyme held in a particular conformation by weak forces of attraction could break on increasing temperature and time. This might result in the 'opening up' of the enzyme permitting an easier approach for the inhibitor to bind to the enzyme, which probably explains the % increase in inhibition.

Table 2: Effect of variable elixir concentration

Elixir	% inhibition
Concentrated	98± 0.5
50 (1:1 diluted)	98±0.5
25	70±0.5
10	54 ± 0.9

Table 3: Effect of Variable exposure time on % inhibition of enzyme

Time in minutes	% Inhibition [#]
5	54.23
10	52.15
20	51.07
30	53.31
40	53.98

*1:10 dilution -Elixir concentration

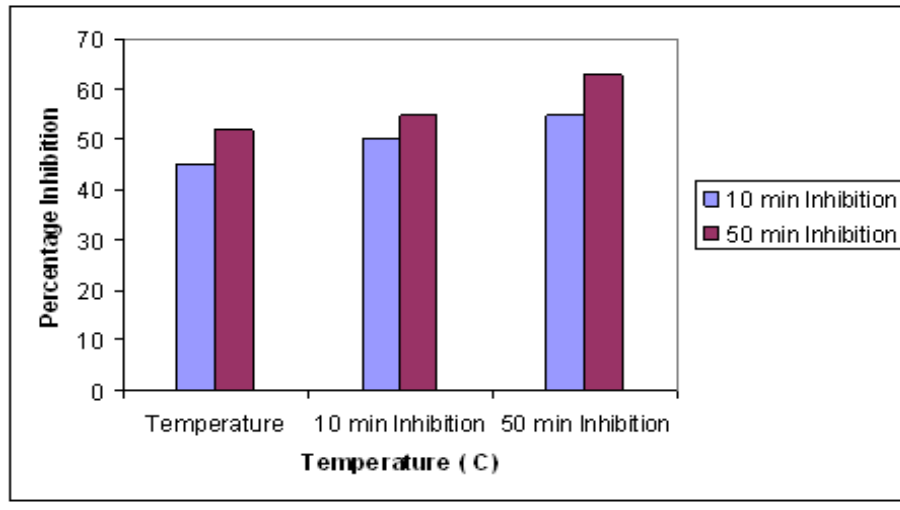


Figure 1: Effect of variable incubation time and temperature on % inhibition of enzyme

Synthesis of B-AuNPs and B-AgNPs

An instant change in colour from light yellow to red indicated the formation of B-AuNPs. Within 1-2 mins the whole solution becomes red. In the case of AgNPs, after 15 mins in room temperature, the appearance of a yellowish colour in the solution indicated the formation of B-AgNPs.

UV-vis Spectroscopy

The curve in Figure 2A shows the presence of surface plasmon resonance (SPR) at 520 nm, characteristic for B-AuNPs. The reduction was very rapid (approx. 1-2 min) as indicated by the clear and characteristic SPR. Similarly, UV-vis spectrum was recorded from B-AgNPs synthesized from 10^4 M AgNO_3 (Figure 2B). The characteristic SPR at 425 nm confirms the presence of B-AgNPs.

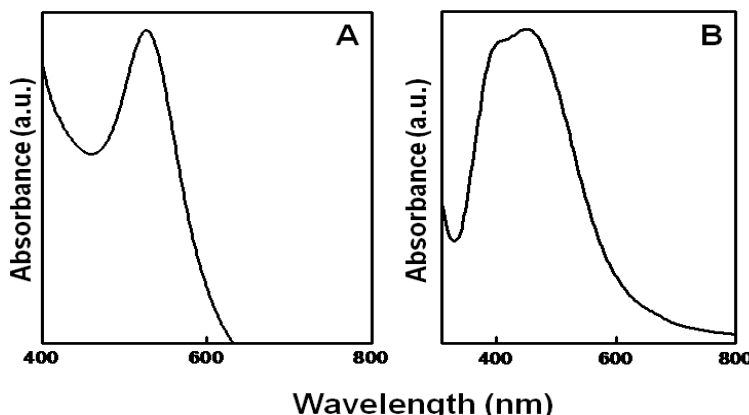


Figure 2: UV-vis spectra recorded from B-AuNPs (A) and B-AgNPs (B).

Transmission Electron Microscopy

Figure 4 (A and B) represents the TEM images obtained from B-AuNPs. The presence of different shapes and sizes of gold nanoparticles can be observed. Polyols present in plant extracts are known to direct the shape of nanoparticles towards more anisotropic structures. The same can

be visually seen in the TEM images. The average size of all the particles remains to be less than 70 nm. Similarly, TEM images of B-AgNPs can be seen in Figure 3 (C and D). It is evident that the particles formed do not conform to any particular shape or symmetry, but are varied in nature.

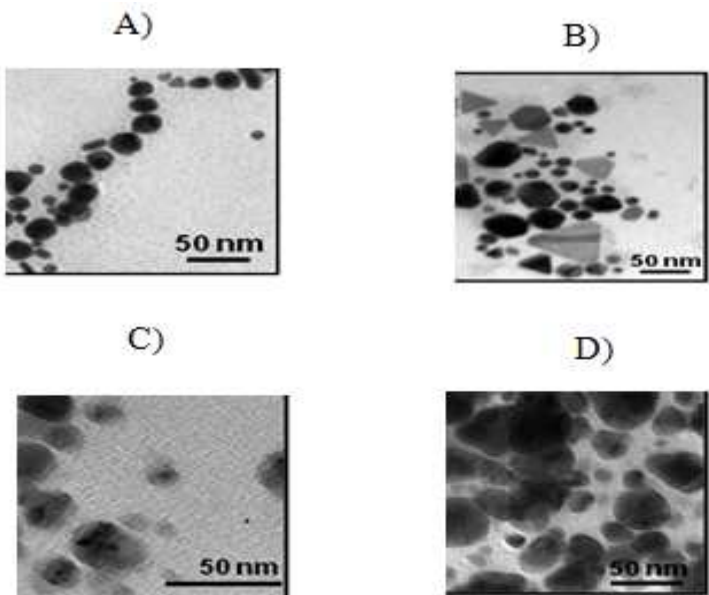


Figure 3: TEM images obtained from B-AuNPs (A and B) and B-AgNPs (C and D)

X-ray Diffraction analysis

The X-ray Diffraction spectra obtained from B-AuNPs and B-AgNPs (Figure 4) show the appearance of peaks corresponding to the (111), (200), (220) and (311) planes characteristic of AuNPs (Figure 4, trace A) and AgNPs (Figure 4, trace B) and thus, proving the crystalline nature of these nanoparticles.

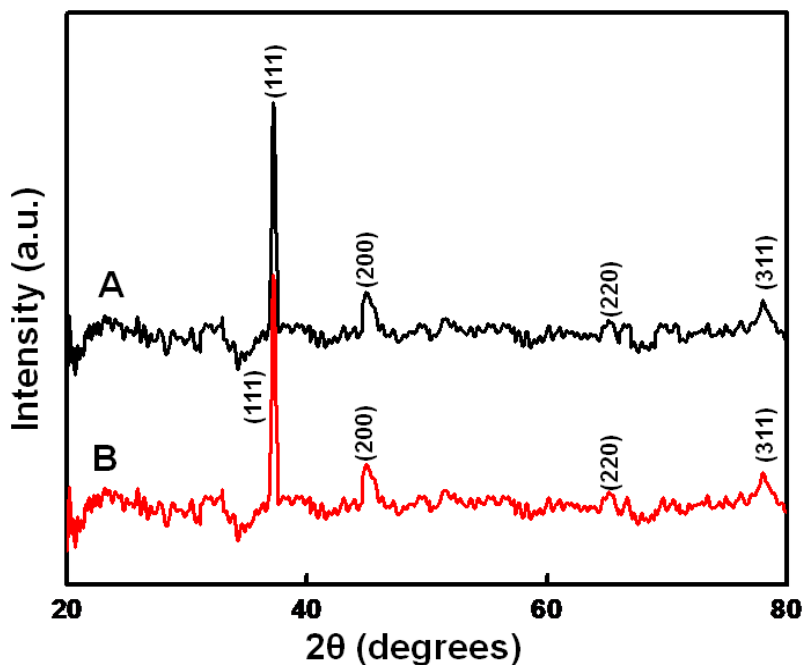


Figure 4: XRD spectra recorded from B-AuNPs (A) and B-AgNPs (B)

Thermogravimetric analysis

Figure 5A clearly indicates that the weight loss takes place in two major regions in the case of B-AuNPs. The first region appears around 200 °C (~30% weight loss) and the second region around 330 °C (~40% weight loss) thus corresponding to

total weight loss of 70%. In case of B-AgNPs (Figure 5B), the weight loss occurs in three regions, the first at 150 °C (~5% weight loss), and the second at around 250 °C (~10% weight loss) and the third one around 375 °C (~15% weight loss) giving a total weight loss of 30%.

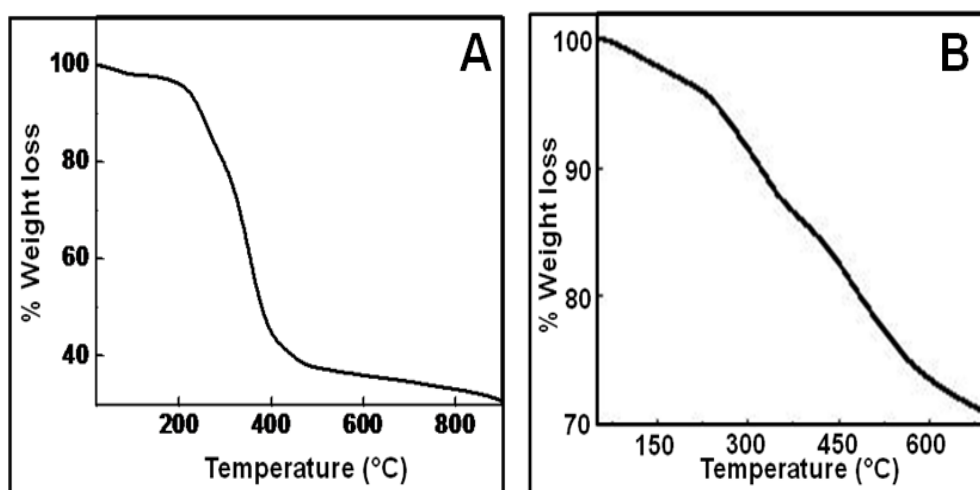


Figure 5: TGA data recorded from A) B-AuNPs showing 70% weight loss and B) AgNPs, showing 30% weight loss

MTT Assay of B-AuNPs

As it is very clear from Figure 6 that B-AuNPs show negligible toxicity to HepG2 cells at all the concentrations used in the experiment. More than 90 % mitochondrial activity was recorded for each concentration. This finding could also be confirmed by the phase contrast microscope images of HepG2 cells taken after the incubation with B-AuNPs. Figure 7 B, C, D and E are HepG2 cell images taken after the treatment with 0.0001 $\mu\text{g}/\text{mL}$, 0.1 $\mu\text{g}/\text{mL}$, 1 $\mu\text{g}/\text{mL}$ and 10 $\mu\text{g}/\text{mL}$ of B-AuNPs respectively, which show cell morphology similar to untreated (Figure 7A) HepG2 cells. HepG2 cells with elongated and well intact morphology adhered to the culture plate surface could be seen even after B-AuNPs treatment.

The phase contrast image of HepG2 cells treated with 100 $\mu\text{g}/\text{mL}$ B-AuNPs (Figure 7F) showed

very few viable cells, as only cell debris could be seen and therefore concentrations above 10 $\mu\text{g}/\text{mL}$ were not taken for the experiments. Aggregates of B-AuNPs can be seen in the form of dark patches spread over a wide area.

The optical image of HepG2 cells treated with 10 $\mu\text{g}/\text{mL}$ B-AuNPs (Figure 7E) do not show much change in cell morphology, indicating that there is no cytotoxic effect of B-AuNPs as the corresponding MTT result shows ~ 100 % cell survival. The increased % mitochondrial activity observed could be due to the contribution of B-AuNPs which also show absorbance in the same range. Therefore it could be concluded here that B-AuNPs at concentrations 10 $\mu\text{g}/\text{mL}$ and below are non-cytotoxic.

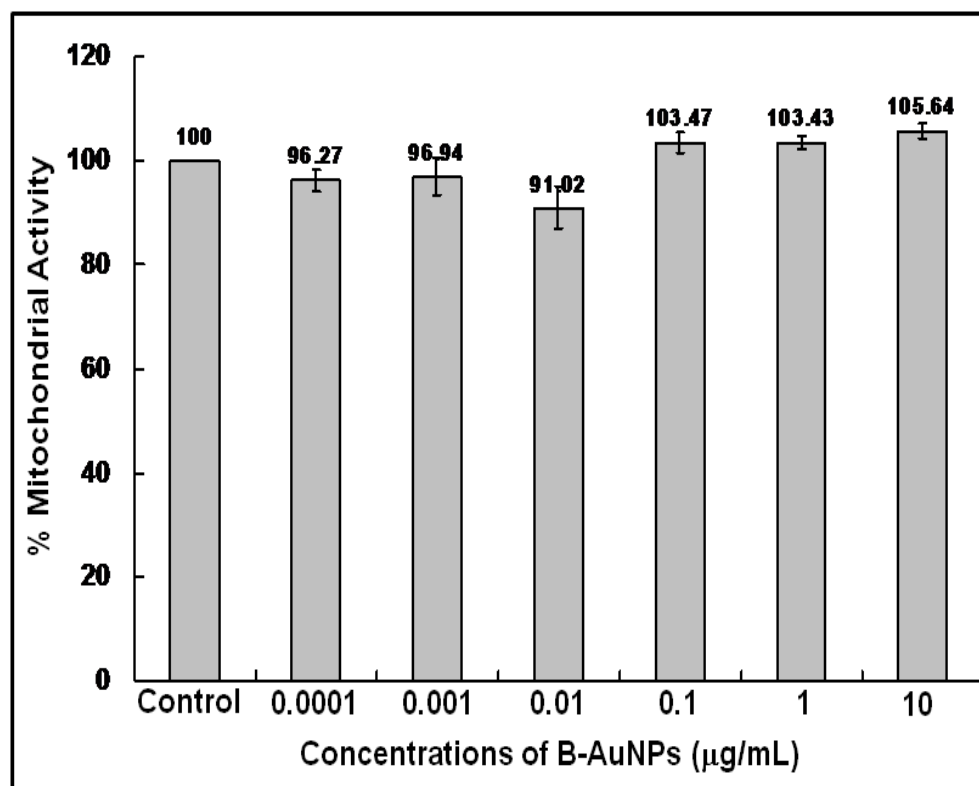


Figure 6: Statistical data representing the % Mitochondrial Activity of human hepatic carcinoma (HepG2) cells after treatment with different concentrations of B-AuNPs for 24 h.

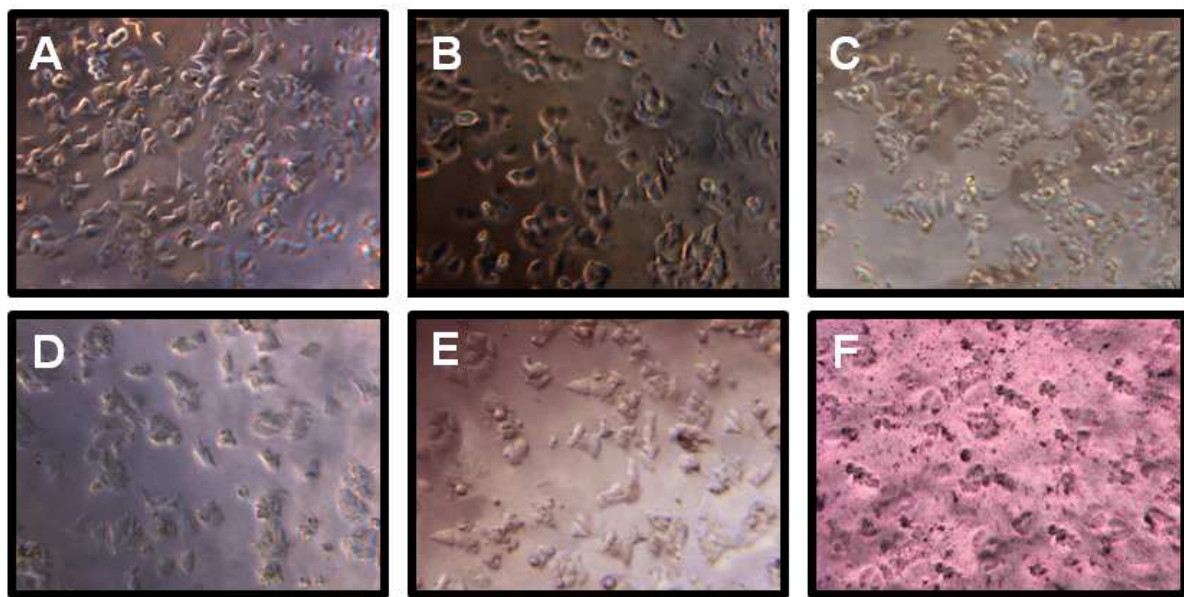


Figure 7: Optical micrographs of HepG2 cells treated with different concentrations of B-AuNPs exposed for 3 h. Figure B, C, D, E and F are images of HepG2 cells after 3 h treatment with 0 µg/mL, 0.0001 µg/mL, 0.1 µg/mL, 1 µg/mL, 10 µg/mL and 100 µg/mL of B-AuNPs. Figure A shows the morphology of untreated (control) cells of HepG2 cells incubated for 24 h.

COMET Assay of B-AuNPs

Though, MTT assay results show that nanoparticles below 10 µg/mL concentration do not show any significant toxicity, it becomes important that we study the genotoxic effects of the same concentration. Cytotoxicity assessment is a way to record the immediate response of cells which come in contact with a foreign material whereas the genotoxicity assessment reveals a long-term response. Thus, it is important that we investigate the genotoxicity of those concentrations that do not actually show any cytotoxicity. Figure 8A shows the % tail DNA pattern of HepG2 cells treated with different concentrations of B-AuNPs. The % tail DNA value for control cells was recorded to be 4.95 units. There was a very slight increase seen in the samples treated with nanoparticles showing values of % tail DNA at 5.58 units, 5.43 units and 5.97 units corresponding to 0.0001 µg/mL, 0.1 µg/mL and 1 µg/mL of B-AuNPs. Further, the resultant comet pattern from the HepG2 cells also show an intact head and complete absence of DNA fragments in the form of tail (Fig. 8 b, c, d and e), suggesting that these doses are not genotoxic. However, B-AuNPs at 10 µg/mL concentration show increase in % tail DNA (6.11 unit) when compared with control (4.95 unit). This increase in % tail DNA pattern was also found non-significant when analyzed with ANOVA. This can

also be concluded from the fact that EMS, the positive control, displays a % tail DNA corresponding to 33.2 units.

Similarly, Figure 9B shows the OTM values recorded from the DNA of HepG2 cells after the treatment with different concentrations of B-AuNPs (0 µg/mL, 0.0001 µg/mL, 0.1 µg/mL, 1 µg/mL and 10 µg/mL) for 3 h. All concentrations do not show any significant increase in OTM (0.77 unit, 0.78 unit, and 0.79 unit) when compared with OTM of control cell (0.73 unit). However, OTM pattern of HepG2 cells treated with 10 µg/mL of B-AuNPs shows an increase in OTM (0.93 unit) as compared to control (0.73 unit). From the analysis by ANOVA, this dose was not found to be significantly toxic. This suggests that even though slight DNA damage occurs at this concentration, it is very minute and cannot be considered as toxic. The corresponding OTM value for EMS treated cells was found to be 8.46 units. This is again confirmed by the comet pattern of the cell DNA (Fig. 8 a-e) showing the entire DNA present in the head. From comet pattern of cell DNA (Fig. 8 e), it is clear that 10 µg/mL concentration of B-AuNPs show little DNA damage, as most of the DNA is intact in the form of comet head and looks similar to control COMET pattern (Fig. 8 a). This result again confirms our MTT observation.

As per COMET assay guidelines (Tice RR, 2000) and based on our MTT observations, concentrations of B-AuNPs above 10 $\mu\text{g}/\text{mL}$ were not used. Further, it may not be necessary to study

the genotoxicity, if the cells are already dead due to cytotoxicity.

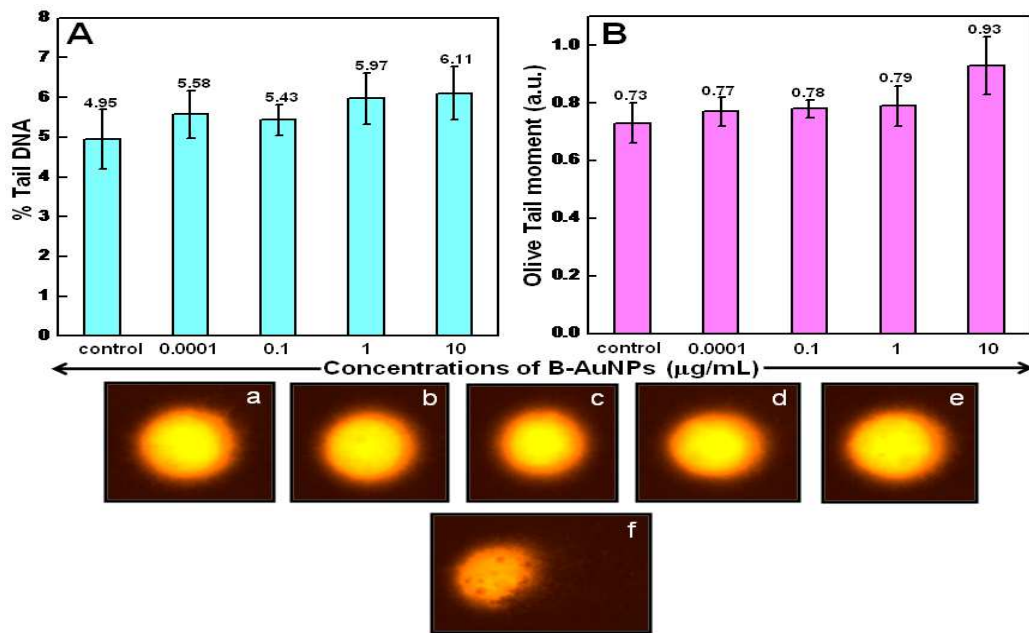


Figure 8: COMET results obtained from 3 h exposure of HepG2 cells with different concentrations of B-AuNPs. Two comet parameters, % tail DNA (A) and Olive tail moment (B) were considered as measure of DNA damage. Figure a, b, c, d and e are images of comet showing the pattern of DNA after the exposure of HepG2 cells to 0 $\mu\text{g}/\text{mL}$, 0.0001 $\mu\text{g}/\text{mL}$, 0.1 $\mu\text{g}/\text{mL}$, 1 $\mu\text{g}/\text{mL}$ and 10 $\mu\text{g}/\text{mL}$ concentration of B-AuNPs respectively. Figure 'f' represents the comet pattern obtained after treatment with 100 $\mu\text{g}/\text{mL}$ of B-AuNPs.

MTT Assay of B-AgNPs

With similar experimental conditions, MTT assay of B-AgNPs was also performed on HepG2 cells. Figure 9 shows the cytotoxicity (MTT assay) response of HepG2 cells after 24 h treatment with different concentrations of B-AgNPs (0.0001 $\mu\text{g}/\text{mL}$, 0.1 $\mu\text{g}/\text{mL}$, 1 $\mu\text{g}/\text{mL}$ and 10 $\mu\text{g}/\text{mL}$). However, the lower B-AgNPs concentrations (0.0001 $\mu\text{g}/\text{mL}$, 0.1 $\mu\text{g}/\text{mL}$ and 1 $\mu\text{g}/\text{mL}$) showed \sim 80-90 % cell survival, which can again be correlated with the optical images showing cell morphology (Figure 10 B, C and D) with untreated (Figure 10A) cells. HepG2 cells treated with these lower concentrations of B-AgNPs showed almost similar morphological characteristics to untreated cells.

HepG2 cells showed \sim 75 % cell survival when exposed to 10 $\mu\text{g}/\text{mL}$ B-AgNPs. This was further

justified by the phase contrast micrograph of HepG2 cells treated with 10 $\mu\text{g}/\text{mL}$ B-AgNPs (Figure 10E). Cells with regular morphology are seen with a few aggregates. But a 75 % survival obtained with this concentration even after 24 h of exposure clearly indicates that this concentration is not really toxic to the cells. In case of HepG2 cells exposed to B-AgNPs (100 $\mu\text{g}/\text{mL}$) (Figure 10F), very few cells are seen along with lot of dark coloured aggregates; damaged cell remains are quite visible. This concentration was thus not taken for further genotoxicity studies. Therefore, it can be concluded that B-AgNPs upto 10 $\mu\text{g}/\text{mL}$ are fairly biocompatible to HepG2 cells. Thus, they could be safely used for different bio-applications.

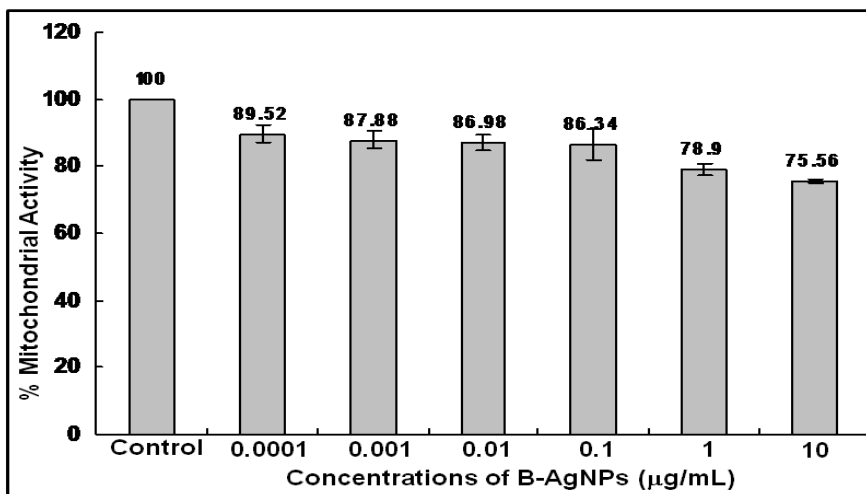


Figure 9: Statistical data representing the % mitochondrial activity of HepG2 cells after treatment with different concentrations of B-AgNPs for 24 h. Details are discussed in text.

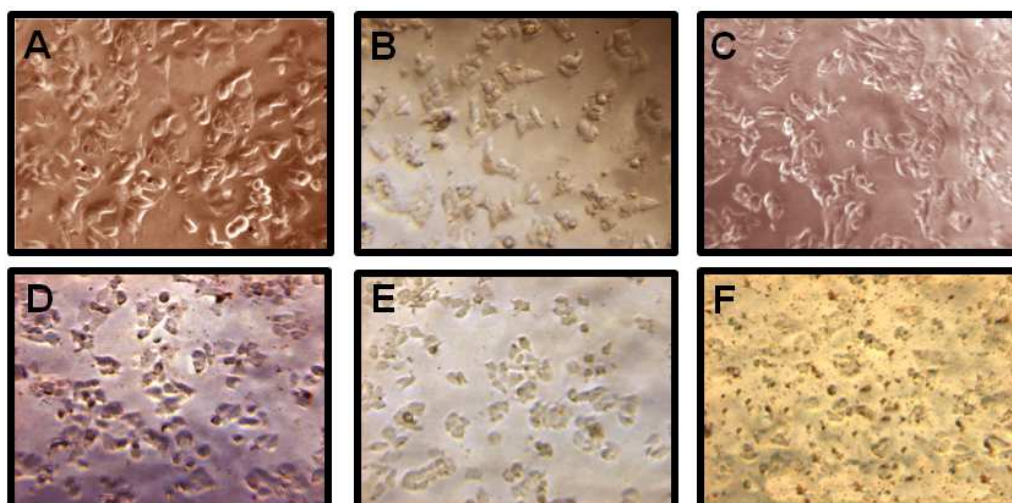


Figure 10: Optical micrograph image of HepG2 cells treated with different concentrations of B-AgNPs exposed for 24 h. Figure B, C, D, E and F are images of HepG2 cells after 24 h treatment with, 0.0001 $\mu\text{g}/\text{mL}$, 0.001 $\mu\text{g}/\text{mL}$, 0.01 $\mu\text{g}/\text{mL}$, 0.1 $\mu\text{g}/\text{mL}$ and 10 $\mu\text{g}/\text{mL}$ of B-AgNPs. Figure A shows the morphology of untreated (control) cells of HepG2 cells incubated for 24 h.

COMET Assay of B-AgNPs

In order to investigate the effect of B-AgNPs on DNA of HepG2 cells, COMET assay was performed in a similar way as was done with B-AuNPs. Here also two COMET parameters (Olive tail moment and % tail DNA) were considered for genotoxicity evaluation.

Figure 11A shows the % tail DNA of HepG2 cells after 3 h of treatment with different concentrations of B-AgNPs (0.0001 $\mu\text{g}/\text{mL}$, 0.1 $\mu\text{g}/\text{mL}$, 1 $\mu\text{g}/\text{mL}$, 10 $\mu\text{g}/\text{mL}$). The lower concentrations of B-AgNPs (0.0001 $\mu\text{g}/\text{mL}$, 0.1 $\mu\text{g}/\text{mL}$, 1 $\mu\text{g}/\text{mL}$) showed % tail DNA values of 4.84 units, 5.11 units and 6.03 units and COMET pattern as untreated cells (4.77 units). However, 10 $\mu\text{g}/\text{mL}$ concentration of B-AgNPs caused an

increase in % tail DNA (6.76 units) as compared to untreated cells (4.77 unit). This increase in % tail DNA was found to be non-significant when analyzed with ANOVA. This suggests that 10 $\mu\text{g}/\text{mL}$ of B-AgNPs causes little DNA damage but this dose cannot be considered as genotoxic. The % tail DNA value of EMS was recorded to be 36.67 units. These results could again be correlated with MTT assay results, obtained after 24 h incubation of HepG2 cells with B-AgNPs (10 $\mu\text{g}/\text{mL}$). The COMET pattern of HepG2 cells treated with 10 $\mu\text{g}/\text{mL}$ concentration of B-AgNPs (Fig. 11 e) also showed well intact DNA head with negligible amount of DNA in the form of tail.

Further, OTM patterns were analyzed after 3 h incubation of HepG2 cells with B-AgNPs.

Here also, lower concentrations ($0.0001\text{ }\mu\text{g/mL}$, $0.1\text{ }\mu\text{g/mL}$, $1\text{ }\mu\text{g/mL}$) showed almost similar amount of OTM (0.77 unit, 0.83 unit and 0.86 unit) as was recorded for untreated cells (0.71 unit). Whereas HepG2 cells treated with $10\text{ }\mu\text{g/mL}$ of B-AgNPs showed increased amount of OTM (0.92 unit) as compared to untreated cells (0.71 unit), which is again non significant under ANOVA analysis. The positive control, EMS, gave a value of 8.98 units. These results were further supported by COMET pattern obtained from respective B-AgNPs treated HepG2 cells (Fig. 11 a, b, c, d and e). Therefore, it could be said that B-AgNPs are non-cytotoxic and non-genotoxic to HepG2 cells up to $10\text{ }\mu\text{g/mL}$ concentration and can be used safely for different applications.

In-order to compare the toxicity due to B-AuNPs and B-AgNPs we must evaluate the amount of nanoparticles present in $10\text{ }\mu\text{g}$ of

nanoparticle sample. According to TGA analysis there is a total weight loss of 70% in case of B-AuNPs which gives $0.6\text{ }\mu\text{M}$ of AuNPs available for interaction. In the same way it has been observed that total weight loss of 30 % in case of B-AgNPs corresponds to $0.8\text{ }\mu\text{M}$ of AgNPs. On comparing MTT data of B-AuNPs and B-AgNPs it was observed that the former gave $\sim 100\%$ cell survival while the latter showed $\sim 75\%$ viability. The values of % tail DNA was also greater in case of B-AgNPs (6.76 units) as compared to B-AuNPs (6.11 units). Although the OTM values in both the cases remain the same. The increased % tail DNA and decreased cell viability in case of B-AgNPs can be attributed to the presence of more amount of silver compared to the amount of gold present in the same weight of B-AuNPs sample. At lower concentrations the nanoparticles in both the cases, showed biocompatibility.

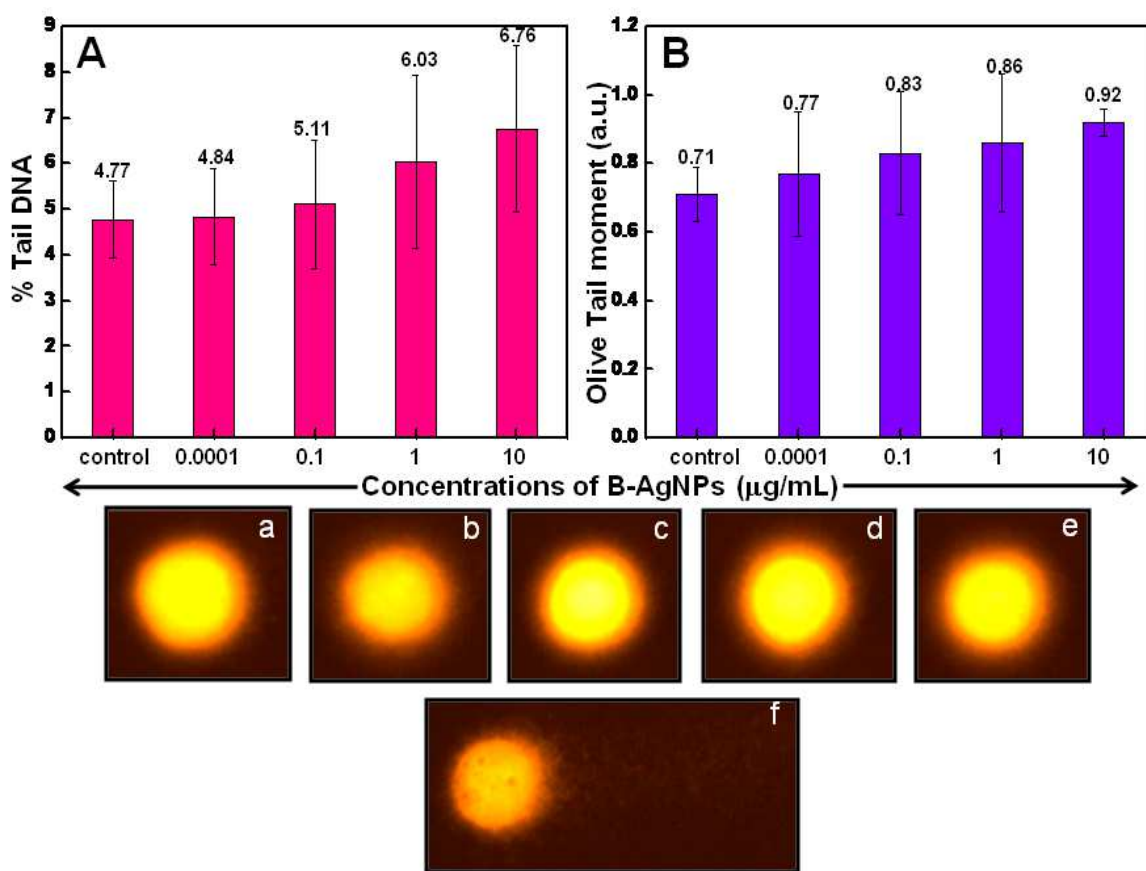


Figure 11: COMET results obtained from 3 h exposure of HepG2 cells with different concentrations of B-AgNPs. Two comet parameters, % tail DNA (A) and olive tail moment (B) was considered as measure of DNA damage. Figure a, b, c, d and e are image of comet showing the pattern of DNA after the exposure of 0 M , 10^{-4} M , 10^{-5} M , 10^{-6} M and 10^{-9} M concentration of B-AgNPs to HepG2 cells respectively.

CONCLUSION

The present paper shows the activity of the enzyme β fructofuranosidase (Invertase) in the presence of diluted and undiluted homeopathic elixir derived from four medicinal plants, *Cephalandra indica*, *Syzygium jambolanum*, *Azardirecta indica* and *Calotropis procera*. The diluted elixir (1:10) showed significant inhibition (above 50%) of invertase activity which was instantaneous. The effect of variable exposure time, incubation time and temperature were studied using this elixir showed that at higher temperatures the enzyme got inhibited more than that when incubated at room temperature..

Nanoparticles synthesized by biological means present better chances of adaptability as compared to their chemically synthesized counterparts. Thus, they can be employed in a variety of bio-applications. As mentioned earlier, many of these applications would bring the

nanoparticles in close contact with mammalian cells and thus it becomes mandatory that a thorough toxicity assessment of these nanoparticles be performed in-order to establish safe and permissible concentrations. Keeping this in mind, we used the above mentioned elixir to synthesize Au and Ag nanoparticles and subjected these nanoparticles to cytotoxicity and genotoxicity evaluation against human liver carcinoma cell lines (HepG2 cells). These nanoparticles showed biocompatibility up to the concentration of 10^{-4} M, which is considerably higher than the reported values. Among B-AuNPs and B-AgNPs, the former showed better biocompatibility within the same concentration exposed to cells. Therefore, they can be safely used for different bio-applications. The results obtained in this study encourage us for further study of these nanoparticles in biomedical applications.

REFERENCES

- [1] Ankamwar B, Damle C, Ahmad A, Sastry M. Controlling the Optical Properties of Lemongrass Extract Synthesized Gold Nanotriangles and Potential Application in Infrared-Absorbing Optical Coatings. *Journal of Nanoscience and Nanotechnology* 2005;5:1665-1671.
- [2] Bilbao C, Ferreiro JA, Comendador MA, Sierra LM. Influence of mus201 and mus308 mutations of *Drosophila melanogaster* on the genotoxicity of model chemicals in somatic cells in vivo measured with the comet assay. *Mutation Research*. 2002; 503: 11-19.
- [3] Chandran SP, Chaudhary M, Pasricha R, Ahmad A, Sastry M. Synthesis of Gold Nanotriangles and Silver Nanoparticles Using *Aloevera* Plant Extract. *Biotechnology Progress*. 2006; 22: 577-583.
- [4] Dunford R, Salinaro A, Cai L, Serpone N, Horikoshi S, Hidaka H, Knowland J. Chemical oxidation and DNA damage catalysed by inorganic sunscreen ingredients. *FEBS Letters*. 1997; 418: 87-90.
- [5] Gardea-Torresdey J L, Parsons JG, Gomez E, Peralta-Videa J, Troiani HE, Santiago P, Jose Yacaman M. Formation and Growth of Au Nanoparticles inside Live Alfalfa Plants. *Nanotechnology Letters*. 2002; 2: 397-401.
- [6] Gascom S and J0 Lampen. Purification of the internal invertase of yeast. *Journal of Biological Chemistry*. 1968; 243:1567-1572.
- [7] Gardea-Torresdey, J. L.; Parsons, J. G.; Gomez, E.; Peralta-Videa, J.; Troiani, H. E.; Santiago, P.; Jose Yacaman, M. Formation and Growth of Au Nanoparticles inside Live Alfalfa Plants. *Nanotechnology Letters*. 2002; 2: 397-401.
- [8] Huang, J.; Li, Q.; Sun, D.; Lu, Y.; Su, Y.; Yang, X.; Wang, H.; Wang, Y.; Shao, W.; He, N.; Hong J.; Chen, C. Biosynthesis of silver and gold nanoparticles by novel sundried *Cinnamomum camphora* leaf. *Nanotechnology*. 2007; 18: 105104-105115.
- [9] Mosmann, T. Rapid colorimetric assay for cellular growth and survival: application to proliferation and cytotoxicity assays. *Journal of Immunological Methods*. 1983; 65: 55-63.
- [10] Nel A, Xia T, Madler L, Li N. Toxic Potential of Materials at the Nanolevel. *Science*. 2006;311: 622-627.

- [11] Nune SK, Chanda N, Shukla R., Katti K, Kulkarni RR, Thilakavathy S, Mekapothula S, Kannan R, Katti KV. Green nanotechnology from tea: phytochemicals in tea as building blocks for production of biocompatible gold nanoparticles. *Journal of Materials Chemistry*. 2009; 19:2912-2920.
- [12] Lakin HW, Curtin GC, Hubert AE, Shacklette HT, Doxtader K G. Geochemistry of Gold in the Weathering Cycle, United States Geological Survey Bulletin. 1974; 1330:1-80.
- [13] Shankar SS, Ahmad A, Sastry M. Geranium Leaf Assisted Biosynthesis of Silver Nanoparticles. *Biotechnology Progress*. 2003; 19: 1627-1631.
- [14] Shankar SS, Ahmad A, Parischa R, Sastry M. Bioreduction of chloroaurate ions by geranium leaves and its endophytic fungus yields gold nanoparticles of different shapes. *Journal of Materials Chemistry*. 2003; 13:1822-1826.
- [15] Shankar SS, Rai A, Ahmad A, Sastry M. Rapid synthesis of Au, Ag, and bimetallic Au core-Ag shell nanoparticles using Neem (*Azadirachta indica*) leaf broth. *Journal of Colloidal and Interfacial Science*. 2004. 275. 496-502.
- [16] Shankar SS, Rai A, Ankamwar B, Singh A, Ahmad A, Sastry M. Biological synthesis of triangular gold nanoprisms. *Nature Material*. 2004. 3. 482-488.
- [17] Shankar SS, Rai A, Ahmad A, Sastry M. Controlling the Optical Properties of Lemongrass Extract Synthesized Gold Nanotriangles and Potential Application in Infrared-Absorbing Optical Coatings. *Chemistry of Materials*. 2005;17(3): 566-572
- [18] Sharma NC, Sahi SV, Nath S, Parsons JG, Gardea- Torresdey JL, Pal T. Synthesis of plant-mediated gold nanoparticles and catalytic role of biomatrix-embedded nanomaterials. *Environmental Science and Technology*. 2007; 41: 5137-5142.
- [19] Singh NP, McCoy MT, Tice RR, Schneider EL. A simple technique for quantitation of low levels of DNA damage in individual cells. *Experimental Cell Research*. 1988; 175: 184-191.
- [20] Tice RR, Agurell E, Anderson D, Burlinson B, Hartmann A, Kobayashi H, Miyamae Y, Rojas E, Ryu JC, Sasaki YF. Single cell gel/comet assay: Guidelines for in vitro and in vivo genetic toxicology testing. *Environmental and Molecular Mutagenesis*. 2000; 35: 206-221.
- [21] Torresdey JLG, Gomez E, Peralta-Videa JR, Parsons JG, Troiani H, Yacaman, MJ. Alfalfa Sprouts: A Natural Source for the Synthesis of Silver Nanoparticles. *Langmuir*. 2003; 19:1357-1361.
- [22] Ogi T, Saitoh N, Nomura T, Konishi Y. Room-temperature synthesis of gold nanoparticles and nanoplates using *Shewanella* algae cell extract. *Journal of Nanoparticle Research*. 2009; 12: 2531-2539.